

PHASE DOPPLER MEASUREMENTS OF LIQUID AGENT TRANSPORT OVER A HEATED CYLINDER

C. Presser^{*}, C.T. Avedisian[‡], and B.S. Johnson^{*}

^{*} National Institute of Standards and Technology
Gaithersburg, MD 20899-8360, USA
cpresser@nist.gov

[‡] Cornell University
Ithaca, NY 14853, USA
cta2@cornell.edu

ABSTRACT

Experimental results are presented for a well-characterized, droplet-laden homogenous turbulent flow field around a cylindrical obstacle. Liquid agent transport was investigated around an unheated and heated cylinder under ambient conditions. Results for water are reported in this investigation. For the heated case, the cylinder was heated initially to a near-surface temperature of approximately 423 K. Phase Doppler interferometry and visualization techniques were used to explore the thermal effects on droplet surface impingement, vaporization, and transport around and downstream behind the cylinder, by providing information of droplet size and velocity in the vicinity of the cylinder. Results indicated that impinging droplets generally coat the surface with few droplets rebounding back into the free stream. Downstream in the wake region of the cylinder, smaller size droplets (generally, of less than 30 μm) are entrained into the recirculation zone. Near the heated cylinder surface, thermal effects reduce droplet mean size significantly.

INTRODUCTION

The next generation of non-ozone-depleting Halon alternatives include chemical suppressants that have high boiling point temperatures (i.e., $T_b > 330 \text{ K}$) and exist in the liquid phase under high-pressure release or in ambient conditions. Release of these agents in a confined cluttered space results in the dispersal of droplets that either travel along ballistic trajectories, move with the convecting flow, or impact upon nearby solid obstacles. An accurate representation of droplet transport is crucial for the numerical modeling of fire suppression in confined spaces using these agents. To better understand the physics of droplet transport around and behind solid objects, an experimental spray facility was modified to impose controlled grid-generated turbulence on the air stream. From this facility, droplet size and velocity data were obtained for a well-characterized, homogenous droplet-laden turbulent flow field around prescribed obstacles. This experimental effort compliments a numerical effort to develop and validate the subgrid model of the VULCAN computational fluid dynamics (CFD) fire physics code for spray-clutter interactive environments, under development at Sandia National Laboratories [1].

In an earlier investigation, the turbulent flow over cylinders of different diameters at ambient conditions was investigated to provide a baseline flow field characterization of geometric effects on the separated flow past the cylinder [2]. The results of this earlier investigation were then expanded to study droplet transport over a cylinder that was preheated to 423 K, well above the boiling point of the agent, for the same turbulent flow conditions [3]. In these two previous studies, particle image velocimetry was used to obtain the two-dimensional velocity field of the gas stream and droplets. The results of this study indicated that smaller droplets are entrained into the recirculation region behind the cylinder while the larger droplets impact the cylinder surface, accumulate and drip off, rebound off the surface and disperse radially outward into the free stream, and/or are entrained in the free stream and transported around the surface. The flow over the heated cylinder indicated the formation of a vapor layer on the downstream side of the cylinder in the shear region between the recirculation zone and free stream. Vaporization of smaller droplets near the heated cylinder surface suggested an increased probability of vapor, and reduced probability of droplet entrainment into the cylinder wake region.

The results of these earlier studies indicated that droplet surface impact, vaporization, and transport behind the cylinder were dependent on droplet size. Thus, this work focuses on measurement of spatially and temporally resolved droplet size and velocity distributions in the upstream and downstream vicinity of the cylinder, using phase Doppler interferometry (PDI). Water was used as the liquid agent, with two additional agents, 3MTM fire protection fluorocarbons HFE-7100 (with a boiling point of 334 K) and HFE-7000 (with a boiling point of 307 K) to be used at a later date. Several strategies may be used to detect size dependent effects in regions where droplets rebound or vaporize. For example, a droplet near the upstream surface of the cylinder with a negative streamwise velocity (i.e., a droplet transported against the flow) would be indicative of a droplet rebounding off of the cylinder surface, and thus PDI would be used to obtain the associated droplet size. If the size distribution near the heated cylinder surface is devoid of relatively smaller size droplets, as compared to other locations away from the cylinder, then this result may be indicative of the effects of vaporization. These ideas were used in interpretation of the measurements.

EXPERIMENTAL SETUP

TEST FACILITY

A schematic of the test facility is shown in Fig. 1. The facility is oriented so that the flow issues horizontally to allow for the collection of liquid agent that drips off the cylinder, and prevent liquid droplets downstream of the obstacle from falling back upstream into the oncoming flow. The agent used in the present study was water, supplied through a 60° solid-cone, pressure-jet atomizer with a higher concentration of droplets in the center of the spray cone (Delavan* type R-D nozzle with a nominal flow rate of 3.0 kg/h at

* Certain commercial equipment or materials are identified in this publication to specify adequately the experimental procedure. Such identification does not imply recommendation or endorsement by the National Institute of Standards and Technology, nor does it imply that the materials or equipment are necessarily the best available for this purpose.

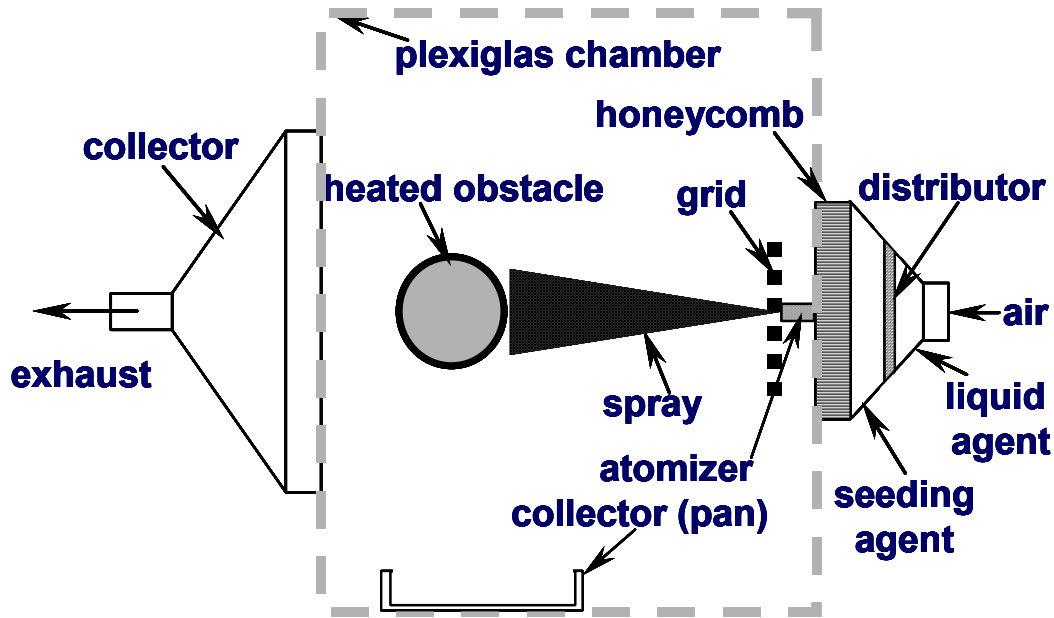


Figure 1. Schematic of the experimental arrangement for the droplet-laden, grid-generated turbulent flow field.

791 kPa). An octagon-shaped Plexiglas insert (with a wall thickness of 6 mm, length of 610 mm, and major and minor axes of 760 mm and 560 mm) was used as a boundary condition. The Plexiglas insert, along with the front face that supported the inlet passages for the liquid agent and air, and back face that supported the exhaust passage, served to form a closed system. A honeycomb layer (51 mm thick with 3 mm size cells) was used to straighten the airflow, which was co-positioned around an injector for the agent (see Fig. 2). Grid generated turbulence was imposed on the air stream by placing a square layer of wire mesh screen (with dimensions of 229 mm width by 330 mm length, 3.2 mm wire thickness, and 13 mm size cells) downstream of the honeycomb. The rationale for this arrangement is given elsewhere [2,3]. For the present experiments, the incoming air (supplied at 265 kg/h) was directed entirely through a distributor plate with steel wool, the circular cross-sectional area of the honeycomb (203 mm in diameter), and then through the wire mesh screen (placed 25 mm downstream of the honeycomb), as shown in Fig. 1. The face of the liquid atomizer was placed flush with the upstream side of the grid, and centered within one mesh cell so that the liquid spray would be unimpeded by the grid. Figure 2 presents a photograph of this arrangement. The integral and Kolmogorov length scales of turbulence were estimated to be approximately 3 cm and 100 μm , respectively. A stepper-motor-driven traversing system translated the entire assembly, and permitted measurements of the flow field properties at selected locations downstream of the injector and around the obstacle.

OBSTACLE CHARACTERISTICS

The obstacle was an aluminum cylinder with a diameter of approximately 29.2 mm and a length of 305 mm (see Fig. 3). Its diameter was larger than the integral length scale of turbulence. A hole (13 mm in diameter) was bored through the center to accommodate

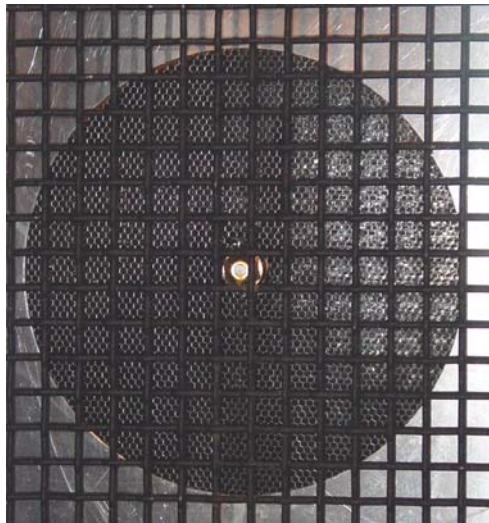


Figure 2. Photograph of liquid atomizer placement in relation to honeycomb and wire mesh screen.

a 250 W cartridge heater (13 mm in diameter and 76 mm in length). The rod was cut along its axis into two halves, and 1 mm deep channels were bored along one segment to accommodate five K-type thermocouples. The thermocouples had an Inconel sheath, were ungrounded, and were 0.8 mm in diameter (305 mm long). The thermocouples were placed in a cross pattern in the center of the rod (each separated by a distance along the surface of 6.4 mm, with the thermocouple junctions placed about 3.2 mm of the surface from within bored holes at each location). The central thermocouple was used for temperature control of the heater, which was positioned behind the thermocouples.

PHASE DOPPLER INTERFEROMETER

Since its introduction, phase Doppler interferometry (PDI) [4,5] has been used to characterize sprays in areas such as liquid fuel spray combustion, coal slurry combustion, coatings, pesticides, fire suppression, and others. PDI is an extension of laser Doppler velocimetry that measures droplet size as well as velocity. Phase Doppler techniques involve creating an interference pattern in the region where two laser beams intersect, and results in a region consisting of alternating light and dark fringes. The region where the laser beams intersect is called the probe volume or sample volume. Due to the interference pattern, a droplet passing through the probe volume scatters light that exhibits an angular intensity distribution, which is characteristic of the size, refractive index, and velocity of the droplet. For a droplet with known refractive index, the size and velocity can be determined by analyzing the scattered light collected with several photomultiplier tubes.

The PDI is a single-point (or spatially resolved) diagnostic instrument in that it obtains information about the spray at a single point in space. Only by moving the probe volume

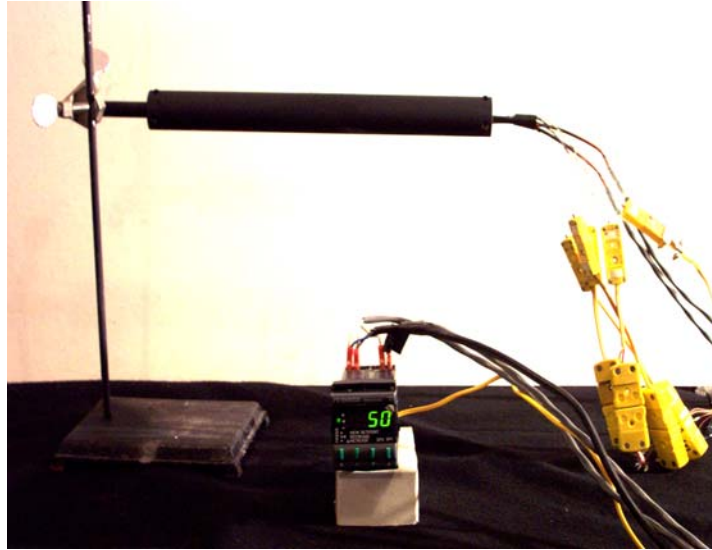
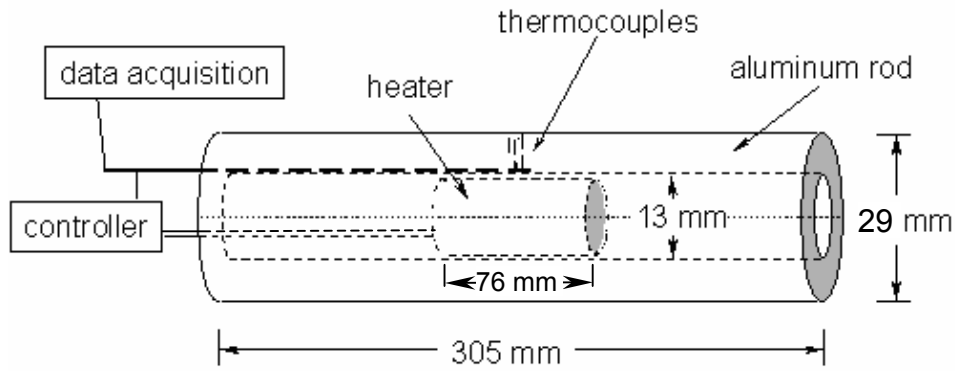


Figure 3. Schematic and photograph of the cylinder with installed cartridge heater

(or, equivalently, the spray) can one map out the spatial distribution of the spray characteristics. The PDI is also a single-particle instrument in that information is obtained for only one droplet at a time. This offers advantages over integrating techniques because the characteristics of a particular droplet (size, velocity, etc.) can be recorded and the data can be separated into classes (size classes, velocity classes) to further characterize the spray system.

The experiments were conducted using a 2-component phase Doppler interferometer with a Real-time Signal Analyzer (RSA) available from TSI, Inc. This PDI system is composed of the following components: (i) transmitter (model XMT204-4.3), (ii) fiber drive (model FBD240-X), (iii) receiver (model RCV216-X), (iv) Real-time signal processors (models RSA3200-P and RSA3200-L), (v) PMT box (model RCM200P), and (vi) RSA IO card v.3.0 (model RSA3CB2DV3). The PDI was controlled using TSI DataVIEW software version 2.02 run on a personal computer using the Windows NT operating system. The RSA has the ability to optimize the number of samples acquired from the Doppler signal in real-time. A 5 W argon ion laser operating in multi-line mode was used as the illumination source. The blue (wavelength = 488 nm) and green (wavelength = 514.5 nm) lines of the argon ion laser were separated by beam

conditioning optics, and focused by the transmitting optics to intersect and form the probe volume. The transmitting optics are coupled to the beam conditioning optics using fiber optic cables to permit the transmitter to be located near the experiment. The front lens on the transmitter has a focal length of 500 mm. The green and blue beams have a beam separation distance of 39.9 mm and 40.2 mm, fringe spacing of 6.45 μm and 6.07 μm , and beam waist of 164 μm and 155 μm , respectively. Frequency shifting is set at

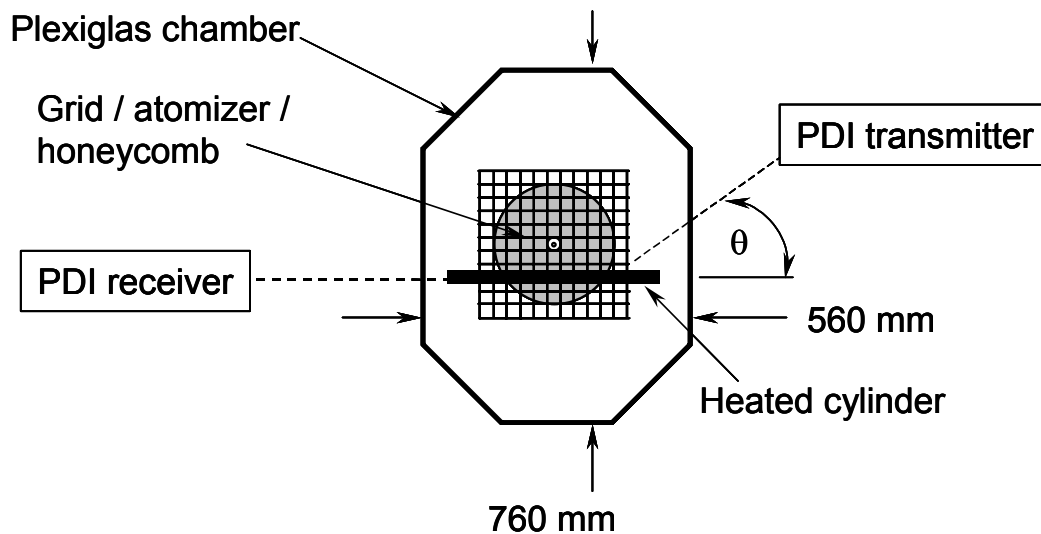
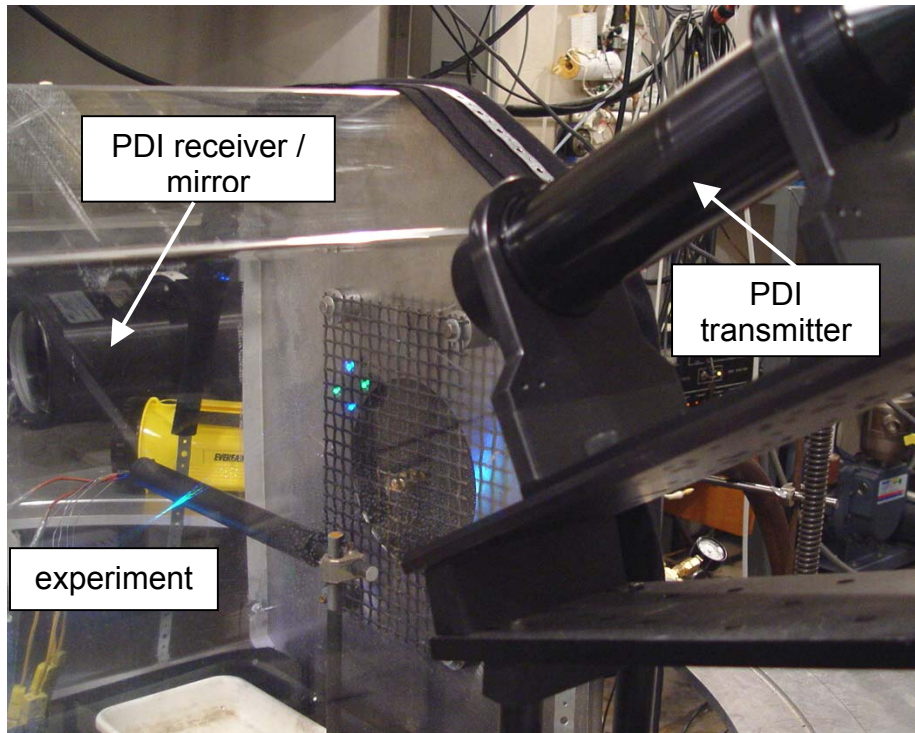


Figure 4. View and schematic of the experimental arrangement with the laser from the phase Doppler interferometry system

40 MHz. The receiver was located at a scattering angle, θ , of 30° measured from the direction of propagation of the laser beams. To accommodate the horizontal orientation of the experimental apparatus, the transmitter and receiver are positioned in a vertical plane, as shown in Fig. 4. Due to the large size of the receiver, the transmitter is positioned with the laser beams angled at 30° to the cylinder, which requires correction of the cross-stream velocity. The front lens on the receiver had a focal length of 1000 mm. The spacing for the three PMT detectors (*A*, *B*, and *C*) that are used to carry out the sizing measurements was 34.8 mm for detectors *A* and *B*, and 101 mm for detectors *A* and *C*. A 150 μm slit aperture is located within the receiver to limit the length of the probe volume.

The signal processor was operated with the following settings: sample frequency of 40 MHz (the rate at which the Doppler signal is sampled), mixer frequency of 36 MHz (mixers are used to reduce the signal frequency prior to analog-to-digital conversion), and a low pass filter setting of 20 MHz (low pass filters are used to remove the summed components from the downmixed signal, so that only the difference is used). The settings result from optimizing the processor for the expected Doppler frequency, which is governed by the droplet velocity and fringe spacing. Hardware coincidence, which requires that droplets be detected on both PDI channels simultaneously to be validated, was used as an additional validation criterion for all measurements. Intensity validation (to remove particles whose scattered light intensities are too low and high, and result in erroneous phase shifts and particle sizes), and probe volume corrections (to account for droplets of varying size traveling through different sections of the Gaussian beam profile) were carried out to optimize the quality of the measurements. The measurements were carried out at several radial (*R*, cross-stream) positions and over a range of axial (*Z*, streamwise) positions upstream and downstream of the cylinder. Figure 5 illustrates the measurement grid that was used and the location of the cylinder relative to the grid mesh. Measurements were carried out from approximately 50 mm upstream of the cylinder to a downstream position of 100 mm. An increment of 2.5 mm was used for $-25.4 \text{ mm} < Z < 38.1 \text{ mm}$, and an increment of 12.7 mm for all other axial positions. In the radial direction, measurements were carried out in increments of 5 mm from 0 to 20 mm in the upper hemisphere (i.e., in the positive radial direction).

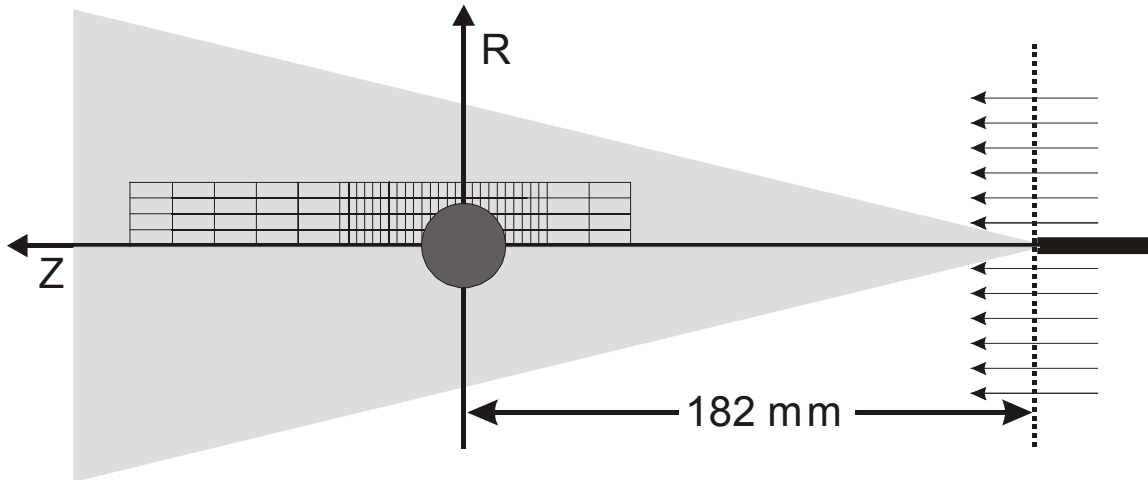


Figure 5. Schematic of the measurement grid around the cylinder

RESULTS AND DISCUSSION

EXPERIMENTAL OBSERVATIONS

In our earlier investigation [3,6], the droplet-laden flow field over both the unheated and heated obstacle was recorded with a high-resolution digital camera (providing both still-images and movies at 9 frames/s). Droplets were observed in the center of the spray impinging on the surface of the cylinder and dripping off at the bottom of the cylinder, while those droplets at larger radial positions were transported around the cylinder. Movies obtained with a high-speed digital camera at 1000 frames per second indicated that many impinging droplets rebounded off of the surface and into the free stream. More rebounding droplets were observed when the air velocity was zero. Few larger size droplets were observed behind the cylinder in its wake, but were abundant with smaller size aerosol droplets that were introduced to the flow through the air stream. There was no evidence of secondary breakup of the droplets, which was expected because the Weber number was much smaller than the critical value for droplet shattering.

When the cylinder was heated to 423 K (i.e., well above the boiling point of water), the droplet-laden flow over the cylinder appeared to be similar to the unheated case except along the shear layer downstream of the cylinder. In this region, a vapor layer formed which was presumed to be the result of vaporization of the liquid that wets the hot surface. It was expected that vaporization of liquid near the cylinder surface may influence locally the transport of droplets behind the cylinder by vaporizing the smaller size droplets, and thus was a focus of the current investigation.

In this study, a solid-cone nozzle was used to increase the number of droplets impinging on the cylinder surface (a hollow-cone atomizer was used in our previous work). It was observed that drippings off the cylinder occurred at a rate of approximately 6.5 mL/min for the unheated cylinder, while there was no dripping for the heated cylinder due to droplet vaporization. It was also observed by the PDI laser beams, as shown by the



Figure 6. Illumination of the phase Doppler laser beams behind the cylinder

reduced intensity around the beam probe volume in Fig. 6, that the concentration of droplets behind the cylinder was significantly reduced. For the heated cylinder, the cylinder surface temperature varied significantly with time after the spray was introduced to the flow field. However, it is unknown at this time whether these changes are attributable to time-varying changes in the response time of the cylinder heater during droplet impingement, or to some other systemic problem.

DROPLET SIZE AND VELOCITIES MEASUREMENTS

The PDI was used to provide information on: 1) droplets rebounding off the upstream face of the cylinder, 2) vaporization of droplets near the heated cylinder, and 3) the droplet sizes that are entrained into the recirculation region behind the cylinder. The unheated cylinder results for the Sauter mean diameter (D_{32}) and droplet mean streamwise component of velocity (U) are presented in Fig. 7. Note that measurements were carried out to check the spray symmetry over the cylinder. The rectangle located on the abscissa at an axial position of $Z \cong \pm 14.6$ mm represents the location of the cylinder. The expanded uncertainty for D_{32} is $3.8 \mu\text{m}$, and for U is 0.35 m/s, calculated as $2u_c$ (representing a level of confidence of 95%), where u_c is calculated as the largest standard deviation of the mean (among standard deviations of the mean based on two replicates at each measurement location) throughout the measurement domain. The gap in the data for the radial positions $R = 0, 5,$ and 10 mm indicates the presence of the cylinder. For Fig. 7A, the general trends are: 1) a decrease in mean size on the downstream side of the cylinder, as compared to the upstream side, and 2) an increase in mean size with increasing radial distance from the central plane of the cylinder. The latter is indicative of the presence of more smaller size droplets near the center of the spray, in particular at $Z = -50$ mm, which is attributed to the design characteristics of the atomizer. For the droplet mean streamwise velocity (see Fig. 7B), the values increase with decreasing radial position at the upstream position of $Z = -50$ mm. These higher velocities correlate with the smaller droplet mean size near the center of the spray. As the droplets approach

the upstream surface of the cylinder, there is a decrease in the streamwise velocity component and an increase in the cross-stream component (data not shown). There is an

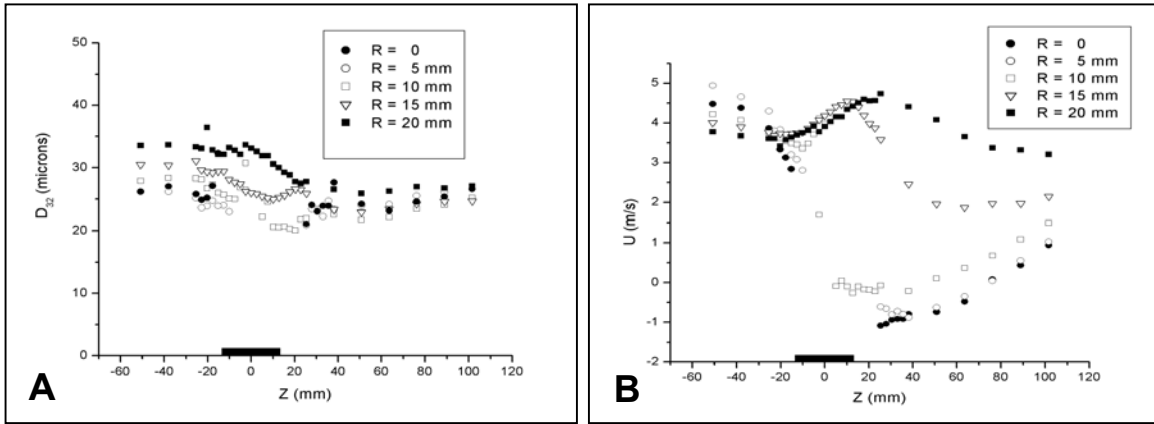


Figure 7. Variation of droplet A) Sauter mean diameter and B) mean streamwise velocity

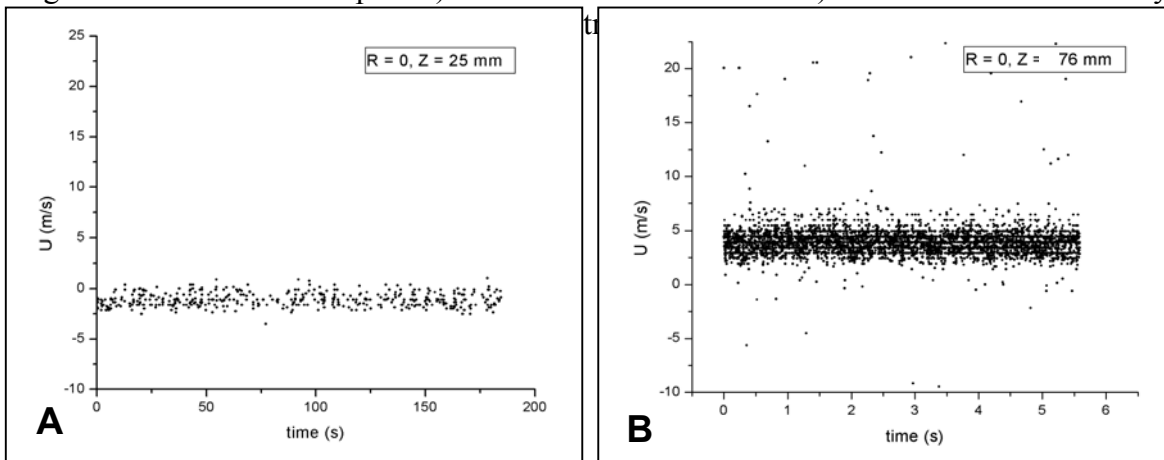


Figure 8. Variation of the streamwise velocity with time at two streamwise positions of A) $Z = 25$ mm and B) $Z = 76$ mm along the centerline, downstream of the unheated cylinder within the recirculation region

increase in the droplet streamwise velocity over the cylinder for $R = 15$, and 20 mm, which was also characteristic of the accelerated flow detected in our earlier PIV investigation [3,6]. At locations near the upstream surface of the cylinder, negative values for the streamwise velocity are detected (data not shown), which may be indicative of droplets rebounding off of the surface. However, positive values of velocity are obtained for the abundance of droplets, which indicates that these impinging droplets either adhere to the cylinder surface or rebound at an angle that maintains their momentum in the downstream direction over the cylinder. The droplet streamwise velocities decrease and become negative values for $R = 0$, 5 , and 10 mm on the downstream side of the cylinder, which is indicative of the presence of a recirculation zone and the entrainment of these droplets into this zone. Data were not obtained immediately downstream of the cylinder (i.e., for ≈ 25 mm $< Z < 14.6$ mm) because the signals were too low to detect any droplets.

Although the magnitude of the droplet mean streamwise velocity downstream of the cylinder is negative, indicating the presence of a recirculation region, it is clear that the mean is representative of a distribution of velocities and associated droplet sizes. This point is highlighted in Fig. 8, which presents the droplet streamwise velocity with respect to droplet interarrival time into the probe volume at two points downstream of the cylinder within the recirculation region. One measurement location along the centerline, at $Z = 25$ mm, represents a measurement close to the cylinder, while the other, at $Z = 76$ mm (see Fig. 8B), represents a location near the downstream edge of the recirculation pattern. The results for $Z = 25$ mm (see Fig. 8A) indicate that many droplets are recirculated upstream toward the cylinder (because $U < 0$), as expected, but also indicate that several droplets at this location are transported in the downstream direction (i.e., $U > 0$). One can speculate that these latter droplets either originate in the recirculation zone or are transported around the cylinder surface and penetrate directly into the recirculation region. The cross-stream velocity component indicates that both positive and negative values are obtained for this group of droplets. In addition, the droplet size does not provide additional information since the size for these droplets varies between $5 \mu\text{m}$ and $30 \mu\text{m}$, and this range is similar to that for the size distribution for the entire population for this measurement. In a similar vane, the results in Fig. 8B indicate that the abundance of droplets are transported in the downstream direction at this point (i.e., for $U > 0$). However, a few droplets are entrained into the recirculation region (i.e., for $U < 0$).

Comparison of results for the unheated and heated cylinders indicates consistently that the droplet Sauter mean diameter, D_{32} , is smaller for the heated case as the droplets are transported past the cylinder surface. The droplet streamwise and cross-stream components of velocity are also lower for the heated case. The unheated and heated results are compared in Fig. 9 for D_{32} and U at $R = 20$ mm. The decrease in the values of both D_{32} and U for the heated case indicates that droplet vaporization does not result in the complete removal of the smaller size droplets from the distribution, but instead a decrease in the size of all droplets (which results in an overall decrease in both the mean size and velocity). In fact, the droplet size distributions illustrate clearly the shift of the entire distribution to smaller sizes for the heated cylinder. An example of this change in the size distributions is given in Fig. 10 at $R = 20$ mm and $Z = 0$.

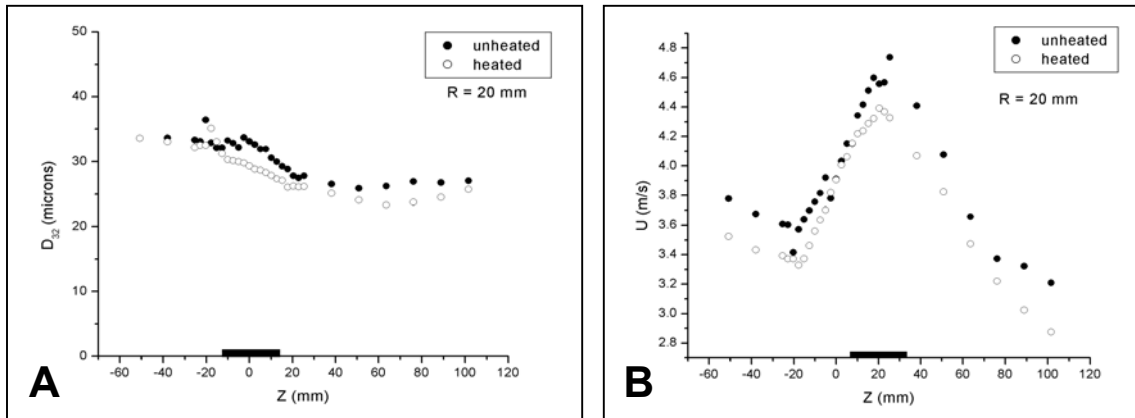


Figure 9. Variation of droplet A) Sauter mean diameter and B) mean streamwise velocity for the unheated and heated cylinders

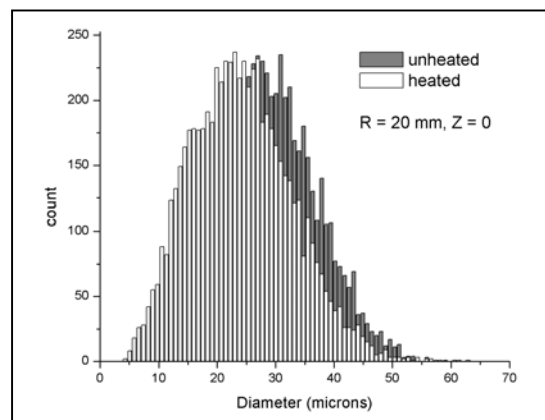


Figure 10. Droplet size distribution for both the unheated and heated cylinder at $R = 20$ mm and $Z = 0$

CONCLUSIONS

Phase Doppler measurements were carried out to obtain droplet size and velocity distributions in a droplet-laden homogenous turbulent flow field around a cylindrical obstacle. Results indicated that most impinging droplets coat the surface with few droplets rebounding back into the free stream. Rebounding droplets are generally less than $30 \mu\text{m}$, corresponding to the higher probability portion of the size distribution. Downstream in the wake region of the cylinder, a distribution of smaller size droplets (generally, of less than $30 \mu\text{m}$) is entrained in the recirculation zone. Near the heated cylinder surface, droplet vaporization results in smaller mean droplet sizes, as compared to the ambient case.

ACKNOWLEDGEMENTS

The authors wish to acknowledge the partial support of this research by the Department of Defense Next Generation Fire Suppression Technology Program, funded by the DoD Strategic Environmental Research and Development Program. The authors wish to thank J. Hewson, D. Keyser, P. Disimile, and J. Tucker of the NGP Project 6A/1 for the discussions and their guidance. We also wish to thank Dr. J.F. Widmann for his help in setting up the phase Doppler interferometer, and Mr. R. Fink for his technical assistance.

REFERENCES

1. DesJardin, P.E., Presser, C., Disimile, P.J., and Tucker, J.R., "A Droplet Impact Model for Agent Transport in Engine Nacelles," Proc. Halon Options Technical Working Conference (HOTWC-2002), New Mexico Engineering Research Institute, Albuquerque, NM, on CD, 2002.
2. Presser, C., Widmann, J.F., DesJardin, P.E., and Gritz, L.A., "Measurements and Numerical Predictions of Liquid Agent Dispersal Around Solid Obstacles," Proc. 11th Halon Options Technical Working Conference (HOTWC-2001), New Mexico Engineering Research Institute, Albuquerque, NM, pp. 122-130, 2001.
3. Presser, C., Widmann, J.F., and Papadopoulos, G., "Liquid Agent Transport Around Solid Obstacles," Proc. 12th Halon Options Technical Working Conference (HOTWC-2002), NIST Special Publication 984 (R.G. Gann and P.A. Reneke, Eds.), NIST, Gaithersburg, MD, on CD, 2002.
4. Bachalo, W.D., and Houser, M.J., "Development of the Phase/Doppler Spray Analyzer for Liquid Droplet Size and Velocity Characterizations," AIAA/SAE/ASME 20th Joint Propulsion Conference, Cincinnati, OH, June 1984.
5. Bachalo, W.D., and Houser, M.J., "Phase/Doppler Spray Analyzer for Simultaneous Measurements of Droplet Size and Velocity Distributions," Optical Engineering, Vol. 23, pp. 583-590.
6. Presser, C., Papadopoulos, G., and Widmann, J.F., "Droplet_laden Homogeneous Turbulent Flow past Heated and Unheated Cylinders," 4th ASME/JSME Joint Fluids Engineering Conference, Honolulu, HI, July 2003.